Available online at www.sciencedirect.com

ScienceDirect

Biochimica et Biophysica Acta 1758 (2006) 1768–1776

BIOCHIMICA ET BIOPHYSICA ACTA

BBA

www.elsevier.com/locate/bbamem

Self-association of isolated large cytoplasmic domain of plasma membrane H^+-ATPase from *Saccharomyces cerevisiae*: Role of the phosphorylation domain in a general dimeric model for P-ATPases

W.I. Almeida *, O.B. Martins, P.C. Carvalho-Alves

Instituto de Bioquímica Médica, Centro de Ciências da Saúde, Universidade Federal do Rio de Janeiro, Rio de Janeiro, 21941-590, Brazil

Received 10 March 2006; received in revised form 21 August 2006; accepted 22 August 2006
Available online 1 September 2006

Abstract

Large cytoplasmic domain (LCD) plasma membrane H^+-ATPase from *S. cerevisiae* was expressed as two fusion polypeptides in *E. coli*: a DNA sequence coding for Leu353–Ileu674 (LCDh), comprising both nucleotide (N) and phosphorylation (P) domains, and a DNA sequence coding for Leu353–Thr543 (LCDΔh, lacking the C-terminus of P domain), were inserted in expression vectors pDEST-17, yielding the respective recombinant plasmids. Overexpressed fusion polypeptides were solubilized with 6 M urea and purified on affinity columns, and urea was removed by dialysis. Their predicted secondary structure contents were confirmed by CD spectra. In addition, both recombinant polypeptides exhibited high-affinity 2′,3′-*O*-(2,4,6-trinitrophenyl)adenosine-5′-triphosphate (TNP-ATP) binding (K_d=1.9 μM and 2.9 μM for LCDh and LCDΔh, respectively), suggesting that they have native-like folding. The gel filtration profile (HPLC) of purified LCDh showed two main peaks, with molecular weights of 95 kDa and 39 kDa, compatible with dimeric and monomeric forms, respectively. However, a single elution peak was observed for purified LCDΔh, with an estimated molecular weight of 29 kDa, as expected for a monomer. Together, these data suggest that LCDh exist in monomer–dimer equilibrium, and that the C-terminus of P domain is necessary for self-association. We propose that such association is due to interaction between vicinal P domains, which may be of functional relevance for H^+-ATPase in native membranes. We discuss a general dimeric model for P-ATPases with interacting P domains, based on published crystallography and cryo-electron microscopy evidence.

Keywords: P-type; ATPase; Oligomerization; Yeast; Protein structure; Self-association

1. Introduction

P-type ATPases constitute an important ubiquitous family of enzymes that transport ions or charged molecules across biological membranes, using energy released from ATP hydrolysis [1,2]. Since the first member of this family was discovered about five decades ago [3], the great number of studies dealing with P-ATPases has lead to significant progress in knowledge of these enzymes' functional features, such that a general kinetic model for active ionic transport has been developed (reviewed in [4–6]). Although the recent determination of sarcoplasmic reticulum Ca^{2+}-ATPase (SERCA) tertiary structure [7,8] provides the framework for interpreting kinetic and mutagenesis data in structural terms, but left many fundamental questions remain unanswered [9]. Among them, protein oligomerization and the exact functional unit resident in biological membranes are still controversial subjects.

Dimeric models that explain kinetic behavior of these enzymes are supported by several physicochemical and immunochemical studies dealing with different P-ATPases [10,11]. Even though monomeric P-ATPase can carry out active

Abbreviations: ATP, adenosine triphosphate; ATPase, adenosine-triphosphatase; bp, base pairs; CD, circular dichroism; DTT, dithiothreitol; HPLC, high performance liquid chromatography; LCD, Large cytoplasmic domain; PCR, polymerase chain reaction; PMSF, phenylmethylsulfonyl fluoride; SERCA, sarcoplasmic reticulum Ca^{2+}-ATPase; SDS, sodium dodecyl sulfate; PAGE, polyacrylamide gel electrophoresis; TNP-ATP, 2′,3′-*O*-(2,4,6-trinitrophenyl) adenosine-5′-triphosphate; MOPS, 3-*N*-morpholinopropanesulfonic acid

* Corresponding author. Tel./fax: +55 21 2562 6789.
E-mail address: welington@bioqmed.ufrj.br (W.I. Almeida).

0005-2736/$ - see front matter © 2006 Elsevier B.V. All rights reserved.
doi:10.1016/j.bbamem.2006.08.018

ion transport [12,13], much evidence points to functional multimeric states for several P-ATPases in their native membranes. For example, kinetic studies suggest that oligomeric states are important for transport [14,15], and that dynamic changes in protein–protein interaction occur during catalytic cycle [16], explaining both cooperative kinetic behavior and enzymatic stability [17–19]. In addition, P-ATPase oligomeric structures have been identified by using proteins in native membranes or by proteins reconstituted in phospholipids/detergent micelles, based on different experimental approaches, including X-rays crystallography or microscopy of tubular crystals [20–28], spectroscopic data [19,29,30], radiation inactivation [31–33], immunochemical detection [18], low-angle laser light scattering photometry [34], co-precipitation [17,35], thermal denaturation [36] and others [37]. However, in some cases, the oligomeric complexes observed were conceivably produced by changes in membrane composition or protein conformation due to the choice of purification method or the experimental conditions, and may not reflect real subunit interactions in native forms. Detailed quaternary structure of these enzymes is still unknown and is a subject of much debate.

The Large Cytoplasmic Domain (LCD) of P-ATPases represents 40–45% of the polypeptide α-chain, and contains most of the enzyme's hydrophilic portion, comprising both nucleotide-binding (N domain) and phosphorylation (P domain) sites. Recently, elucidation of SERCA three-dimensional structures has shown that the P domain assumes the Rossman fold motif, formed by the LCD N-terminal beta-sheet containing Asp 351(the residue that is phosphorylated by ATP) surrounded by 50 C-terminal amino acids, before re-entering the membrane [7,8], as suggested by homology modeling with haloacid dehalogenase [38].

Evidence suggesting that LCD plays a critical role in protein oligomerization came first from studies with Na^+,K^+-ATPase [17], and it has been proposed that a 150 amino-acid segment at LCD C-terminus is essential for association of α-subunits [35]. Recently, we have shown that isolated LCD from SERCA (LCD/SERCA), heterologously expressed in *E. coli* as a fusion protein, is unable to form dimers when the equivalent C-terminal portion was removed by proteinase-K treatment [39]. The proteolyzed segment was the P domain and the monomeric segment was identified as the N domain [7]. Thus, expressing and characterizing LCD from other P-ATPase family members is of interest as to address the question of whether P domain is important for protein–protein interaction in this ATPase class as a general rule. Accordingly, we describe cloning, heterologous expression, purification, and structural characterization of both LCDh, a fragment comprising the entire N and P domains of plasma membrane H^+-ATPase from *S. cerevisiae* (*pma*1); and LCDΔh, a truncated LCD fragment lacking the P domain C-terminus.

Our data indicate that P domain is necessary for dimerization of LCDh, as previously shown for LCD/SERCA [39], supporting the hypothesis that such interaction may be of functional relevance for P-ATPases in native membranes. We discuss our data in terms of a general dimeric model for P-ATPases based on crystallography and cryo-electron microscopy.

2. Materials and methods

2.1. Subcloning of LCDh and LCDΔh and construction of expression vectors

The segments corresponding to plasma membrane H^+-ATPase Large Cytoplasmic Domain with (LCDh) and without (LCDΔh) its C-terminus were amplified by PCR with *Pfx*-polymerase, using *pma*1 gene as template (kindly supplied by Dr. Carolyn Slayman, Yale University, USA), and three oligonucleotides (primers): 5′-GGGGACAAGTTTGTACAAAAAAGCAGGCTTCTTGGCTAAGAAACAAGCCATTG-3′ and either 5′-GGGGACCACTTTGTACAAGAAAGCTG GGTCCTAAATAGCAGATAGACC-3′ for LCDh or 5′-GGGGACCACTTTGTACAAGAAAGCTGGGTCCTAAGTTTGAGCAGTATC-3′ for LCDΔh. These primers were designed on the basis of GenBank entry 1168544, *pma*1 gene [40] with the added site-specific recombination (underlines) of phage lambda [41,42] (Invitrogen).

PCR products were subcloned into *att*P sites of pDONR-201 (Invitrogen), yielding either entry clone LCDh (pENTR/LCDh) or entry clone LCDΔh (pENTR/LCDΔh). Direction of insertion was checked by restriction enzyme digestion. DNAs of entry clones were used to transfer LCDh and LCDΔh into destination vector pDEST-17 (which contained a phage T7 promoter; Invitrogen), yielding pDEST-17/LCDh and pDEST-17/LCDΔh, respectively. This vector introduces an amino-terminal hexahistidine tag suitable for Ni^{2+} affinity purification. Recombinant plasmids were transformed into *E. coli*DH5α for DNA cloning and sequencing and BL21-SI (salt inducible) for protein expression [43] (Invitrogen). Gene sequence was confirmed by automated DNA sequence analysis.

2.2. Overexpression, purification and renaturation procedures

Engineered pDEST-17 was used to transform BL21-SI strain. *E. coli* transformants were selected on LB agar without sodium chloride, dubbed LBON [44] which contain ampicillin (100 μg/ml). An overnight culture of 5 ml was prepared and used to inoculate 500 ml of LBON medium containing ampicillin (100 μg/ml). Expression was induced by adding 0.3 M NaCl at an optical density of 0.6–0.7 at 600 nm. After further growth in 150 min, bacteria were collected, suspended in 10 ml of lysis buffer (50 mM sodium phosphate, 1 mM PMSF, pH 7.0), and sonicated at 80 W using 6 pulses of 30 s (Branson/250) on ice. The lysate was then centrifuged, and the pellet was resuspended in 10 ml of extraction buffer (6 M urea, 25 mM sodium phosphate, 200 mM ammonium sulfate, pH 7.5 and 10 mM β-mercaptoethanol) and centrifuged (5,000×*g* for 15 min at 4 °C) . The supernatant was collected (10 ml containing 10 mg protein) and used to load the affinity column.

To purify the engineered polypeptides LCDh and LCDΔh, we used 3 ml Ni-NTA resin pre-equilibrated with extraction buffer. The 6 M urea extract was applied and the column was washed twice with 10 ml of extraction buffer. Fusion polypeptides were eluted with 10 ml of extraction buffer supplemented with 25 mM imidazole for LCDh or 120 mM imidazole for LCDΔh. All protein determinations were performed in accordance with Bradford [45]. Aliquots containing 10–25 μg of LCD polypeptides were used for SDS-PAGE. Protein expressions and purification were examined on 10% SDS-PAGE [46]. Protein bands were observed by staining the gels with Coomassie Brilliant Blue. For Western blotting, the polypeptides were electro-transferred from gels to PVDF membranes (Imobilon-P, Millipore) using 150 mA for 60 min, using the mouse anti-hexahistidine antibody (Sigma) diluted 1/4000. Antibodies were detected using the ECF kit (Amersham, UK).

Refolding of engineered proteins was initiated by a progressive elimination of urea. For this purpose, LCDh and LCDΔh polypeptides were dialyzed for 12 h at 4 °C against decreasing concentrations of urea (4 M, 2 M or no urea) and 25 mM sodium phosphate, pH 7.5, 200 mM ammonium sulfate, 10 mM β-mercaptoethanol, 3 mM DTT. After dialysis the protein was stored on ice. Alternatively, the protein was concentrated 10-fold using an Ultrafree-15 centrifugal filter device (Millipore, Bedford, MA, USA) and the buffer was changed to 20 mM MOPS at the same pH and in the presence of the same salt and reducing agents.

2.3. Circular dichroism

CD measurements were carried out on a J-715 spectropolarimeter (Jasco Corp., Japan), using a 0.1-cm path-length quartz cell. Spectra were obtained in

25 mM sodium phosphate buffer containing 100 mM ammonium sulfate, 10 mM β-mercaptoethanol, and 0.3 mM DTT at pH 7.0, and spectra from buffer alone were subtracted. Three scans from 190 to 260 nm were performed to obtain each spectrum. The units are expressed as molar ellipticity per residue (degree cm^2 $dmol^{-1}$).

Three different algorithms were used to deconvolute CD spectra of proteins using CDPro package [47]. The algorithms used were Selcon, containing 33 proteins in the data base, Contin with 16 proteins in the data base; and CDSSTR. The values found were compared with predicted contents for LCDh and LCDΔh polypeptides, using SOPMA [48].

2.4. TNP-ATP fluorescence measurements

TNP-ATP fluorescence measurements were performed at room temperature in a medium containing 20 mM MOPS pH 7.25, 100 mM KCl, and 0.2 M ammonium sulfate, in a 1 × 1 cm fluorescence cuvette under continuous stirring using a photocounting spectrofluorimeter. The excitation wavelength was 410 nm (bandwidth = 5 nm) and the emission wavelength was 540 nm (bandwidth = 20 nm). Nucleotide binding was measured from the difference of fluorescence intensity in the presence and absence of 1 μM of either LCDh or LCDΔh after correcting for inner filter effect.

2.5. Gel filtration

Gel filtration experiments were carried out by HPLC (Shimadzu, Japan) using a GP 100 column. The flow rate was 0.5 ml/min with eluting buffer (25 mM sodium phosphate, 100 mM ammonium sulfate, pH 7.0). The column was calibrated for molecular mass with α-amylase, albumin, ovalbumin and carbonic anhydrase [49]. Protein elution was monitored by detecting fluorescence emission at 320 nm.

3. Results

The overall aim of our study is to investigate the role of Large Cytoplasmic Domain (LCD) of P-type ATPases in self-association, and in particular, the relevance of C-terminal residues, which compose most of the P domain. For this purpose we subcloned and overexpressed two constructions of LCD from *S. cerevisiae* plasma membrane H^+-ATPase: LCDh (from Leu 353 to Ile 674), which contains both N and P domains; and LCDΔh (from Leu 353 to Thr 543), which lacks the C-terminal portion of the P domain.

3.1. Construction of the E. coli expression vectors

Recombinant plasmids encoding LCDh (about 1000 bp) and the C-terminus-deleted LCDΔh (about 700 bp) were checked by restriction-enzyme digestion and confirmed by DNA sequencing. pENTR clones generated by BP reaction (i.e., recombinant plasmids for insertion of PCR products with *att*B into pDONR-201) were checked with *Ban*II, and recombinant pDEST-17 plasmids, generated by LR reaction were checked with *Eco*RI (data not shown).

3.2. Overexpression and purification of the LCD from H^+-ATPase polypeptides in E. coli

Expression in *E. coli* BL21-SI was induced by 0.3 M sodium chloride. The expected polypeptides bands were observed in SDS-PAGE (35,705 Da for LCDh and 20,994 Da for LCDΔh, Fig. 1A). In both cases, after induced cells were disrupted by sonication, most of the LCD polypeptides appeared as inclusion bodies, which were then solubilized with extraction buffer containing 6 M urea. After centrifugation, to discard the remaining aggregates, the fusion polypeptides were purified on a Ni^{2+} affinity resin (Fig. 1B). Then they were refolded by stepwise dialysis and recovered in soluble form (around 3–5 mg/500 ml of cultured cells).

3.3. CD spectra and binding of TNP-ATP

CD spectroscopy was employed in order to characterize LCD secondary structure (Fig. 2A and B). Table 1 summarizes secondary structure content of each construction based on CD

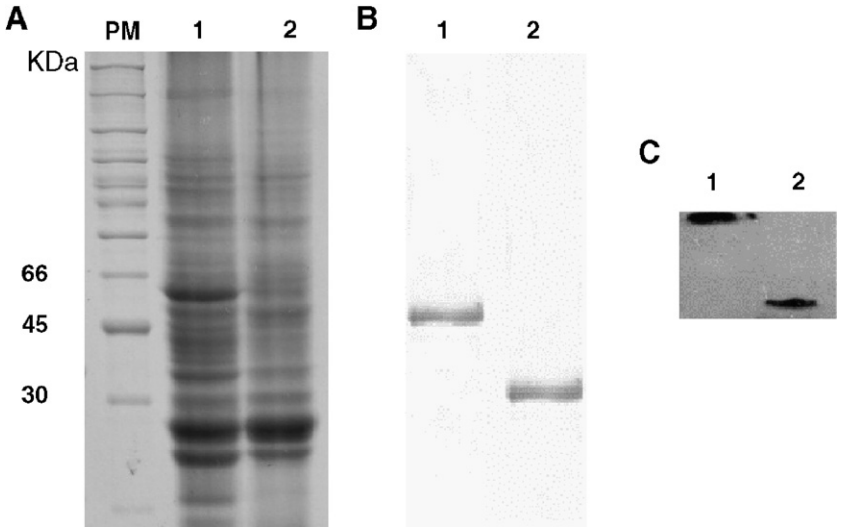

Fig. 1. Purification of LCDs from PMA1. SDS-PAGE of fractions obtained during purification stained with Coomassie Blue. PM, molecular weight standards (molecular masses in kDa, indicated at left); 1, crude extract of the induced LCDh; 2, crude extract of the induced LCDΔh; (B) 1, affinity-column elution of purified LCDΔh (about 21 kDa) with extraction buffer supplemented with 120 mM imidazole; 2, affinity-column elution of purified LCDh (about 36 kDa) with extraction buffer supplemented with 25 mM imidazole; (C) Western blot of LCD polypeptides with anti-hexa-His amino-tag antibody. 1, purified LCDΔh; 2, purified LCDh.

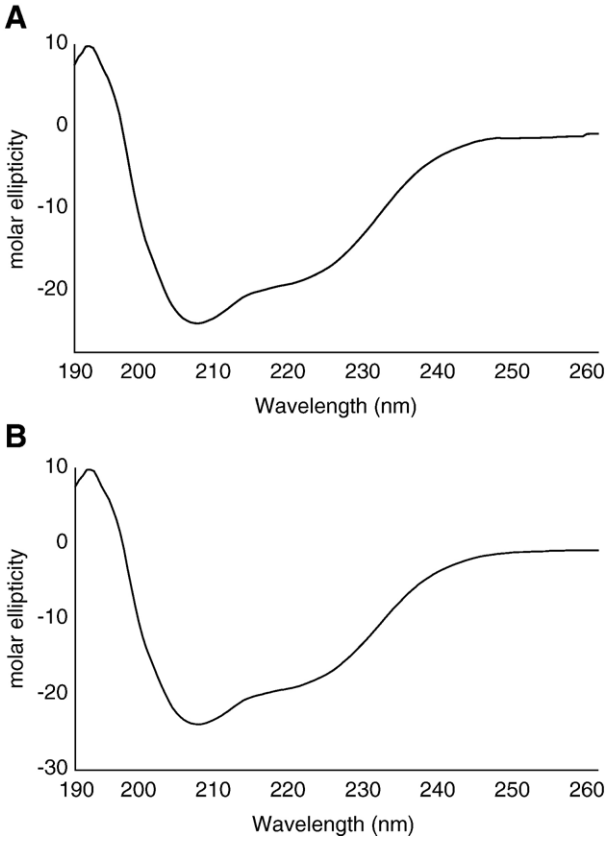

Fig. 2. CD spectra of LCDs from PMA1. (A) Spectrum of LCDh. (B) Spectrum of LCDΔh. Both spectra were obtained in 25 mM sodium phosphate buffer containing 100 mM ammonium sulfate, β-mercaptoethanol and 0.3 mM DTT at pH 7.0. CD measurements were carried out on a Jasco J-715 spectropolarimeter, using an 0.1-cm path-length quartz cell. Molar ellipticity is in deg cm^2 $dmol^{-1}$. Resultant spectra are average of 3 scans.

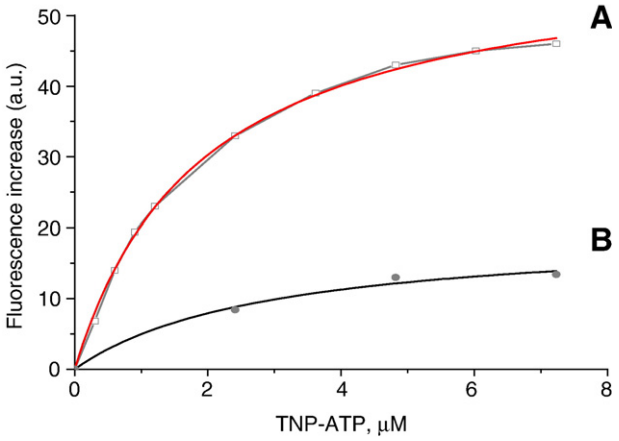

Fig. 3. Binding of TNP-ATP to LCDs from PMA1. TNP–ATP binding was determined by measuring the difference between TNP–ATP fluorescence in the presence of 1 μM LCDh (A) or LCDΔh (B), and in the absence of protein (not shown). Fluorescence increase (F) is represented on an arbitrary scale. The solid lines represent a non-linear fit of data, from where the dissociation constant (K_d) and the maximal fluorescence at saturation (F_{max}) were calculated.

spectrum deconvolution using three different algorithms. These values can be compared with hypothetical contents predicted from LCD polypeptide primary structure using SOPMA. For LCDs from *PMA1*, both α-helix and β-strand contents, obtained from the three deconvolution algorithms were similar to those predicted from primary sequence (44% and 30%, respectively).

TNP-ATP binding affinity was measured by the difference in fluorescence intensity (F) in the presence as opposed to the absence of the polypeptides (Fig. 3). LCDh and LCDΔh bound TNP-ATP with high affinity (K_d=1.9±0.1 μM and 2.9±1.1 μM, respectively). The apparent affinity (K_d) and maximal fluorescence (F_{max}) were obtained by a non-linear fitting of the data from experiments performed in the presence of each polypeptides, assuming a hyperbolic dependence of F on TNP-ATP concentration. These K_d values are very similar to those previously described for the recombinant LCD/SERCA [39] or for the recombinant LCD/PMA [50]. The value of F_{max} calculated for LCDh was 3-fold higher than that calculated for LCDΔh. Together these data suggest that our recombinant LCD polypeptides have a three-dimensional structure very similar to that found in the native H^+-ATPase.

3.4. Association state of LCD polypeptides

The association state of each LCD polypeptide was examined by size-exclusion HPLC. Intrinsic fluorescence emission (at 320 nm) was employed to monitor protein elution. LCDh exhibited two main peaks, with relative molecular masses of 95 and 39 kDa, compatible with dimeric and monomeric forms, respectively (Fig. 4A). On the other hand, LCDΔh showed a monodisperse profile, with a single peak at 29 kDa estimated molecular weight, as expected for monomers (Fig. 4B). The same amount of protein was applied in each case. These data indicate that the C-terminal portion of LCD from PMA1, which is absent in the LCDΔh construction, is necessary to observe protein association. These data are in line with those obtained previously using isolated LCD/SERCA [39].

Table 1
Secondary structure content of LCDs obtained by CD spectra deconvolution

Secondary structure motif	CONTINLL		SELCON 3		CDSSTR		Predicted*	
	LCDh	LCDΔh	LCDh	LCDΔh	LCDh	LCDΔh	LCDh	LCDΔh
Alpha-helix (%)	39	38	43	40	49.5	45	44.3	41.4
Beta-strand (%)	30	30	30	30	29.2	30	27.1	30.4
Other (%)	31	32	27	30	21.3	25	28.6	28.2

Algorithms shown along the top were used for deconvolution of Fig. 2 CD spectra (CDPro package); * predicted refers to fold predicted for LCD peptides using SOPMA.

4. Discussion

This work provides new structural evidence for the relevance of LCD in self-association of P-ATPases, and in particular, the fundamental role of the P site for oligomerization. Oligomeric arrangements of P-ATPases have been proposed for a long time, starting early observations of biphasic dependence on ATP concentration for enzyme activity [10,11]. Before publication of Toyoshima's model [7], attempts to obtain higher resolution structural data resulted in several reports describing over-expression of soluble domains of P-ATPases in *E. coli,* as an alternative approach [50–54]. Those data demonstrated that isolated LCDs are able to bind nucleotides, but crystals suitable for X-ray analysis have never been obtained, nor have the LCD oligomeric states been properly investigated. The first evidence suggesting that LCD is important for P-ATPase self-association came from the observation that Na^+,K^+-ATPase oligomeric complex depended on interactions between α-subunits [17]; more specifically, on a sequence of 150 amino acids located within the LCD C-terminal portion [35]. Later, it was demonstrated that isolated LCD/SERCA, when expressed in *E. coli* as a fusion protein, has a high tendency to form dimers [39]. Interestingly, LCD/SERCA treated with proteinase K generated a monomeric fragment, similar to that produced upon digestion of native ATPase by the same protease [55]. This monomeric peptide core was identified, in the light of Toyoshima's model, as the whole nucleotide binding site (N), devoid of N- and C-terminal sequences that compose the phosphorylation site (P). Thus, LCD/SERCA self-association needs at least part of the P site, as the N site alone does not form dimers [39].

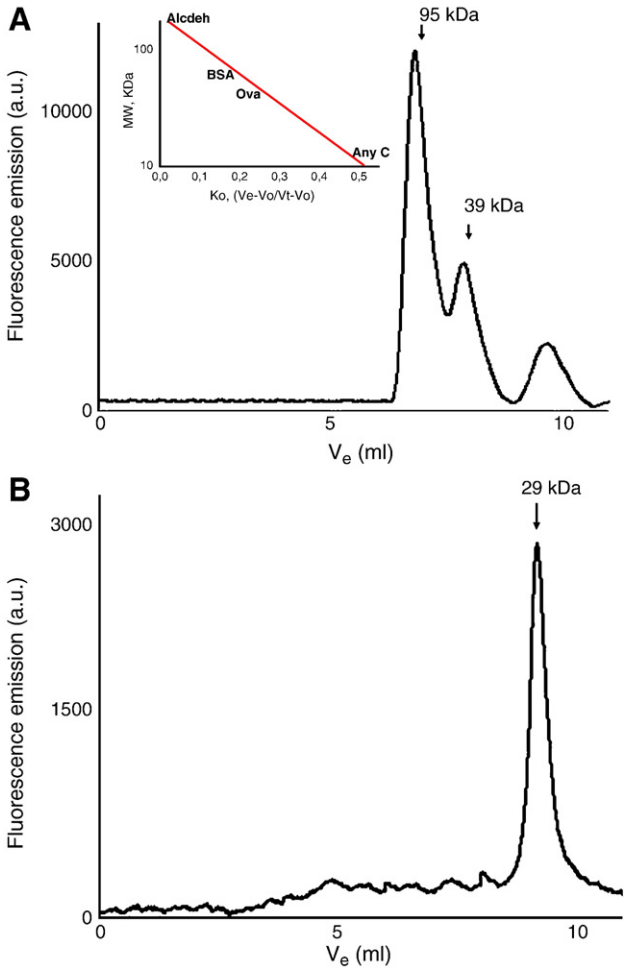

Fig. 4. Size-exclusion HPLC of LCDs. LCDh elution profile (A) shows 2 main peaks (arrows) corresponding to MWs of 95 kDa and 39 kDa, as expected for dimeric and monomeric forms, respectively; while LCDΔh elution profile (B) shows only one peak (arrow) corresponding to MW of 29 kDa, as expected for monomeric form. Elution performed in 25 mM sodium phosphate, 100 mM ammonium sulfate buffer (pH 7.0). The apparent molecular weights of the main elution peaks were estimated by referring to a calibration curve (Inset).

We decided to extend the study with isolated LCD, as fusion protein, to the H^+-ATPase from *S. cerevisiae*, in order to investigate whether it also self-associates and, in this case, whether such association would also be dependent on C-terminal residues of the P site. For this purpose, we have constructed and expressed vectors containing the gene sequence coding for N and P sites (LCDh), or an alternative deleted version without all P site C-terminal amino-acid residues (LCDΔh). As expected, purified LCDh and LCDΔh showed in SDS-PAGE mainly bands of about 36.0 and 21.0 kDa (accounting for about 97% of total protein), respectively (Fig. 1B). CD spectra deconvolution of both purified proteins, after stepwise dialysis (Fig. 2A and B) were consistent with predicted secondary structure contents (Table 1), and therefore we believe that they have folded similarly to native protein. From these data, LCDh would be quite helical (44%), in contrast to either LCD/SERCA, which contains 20–23% α-helix and 21–25% β-sheet [39] or LCD/Na^+,K^+-ATPase, which contains 23% α-helix and 27% β-sheet [52]. Such structural difference between LCDh and other LCDs may be attributed to deletions in the N domain, and may account for PMA1's high specificity for ATP [56], in contrast to SERCA and Na^+,K^+-ATPase, which are known to hydrolyze many different phosphorylated compounds. In addition, we showed that both LCD polypeptides bind TNP-ATP (Fig. 3) with high affinity, a property which is similar to those described for other P-type LCD recombinant constructions [39,50]. These data support the conclusion that the polypeptides have folded into a biologically relevant conformation.

However, the most important result here is the finding that refolded LCDh showed two main fluorescent elution peaks, when analyzed by size-exclusion HPLC, with calculated molecular weights of 95 and 39 kDa, compatible with dimeric and monomeric forms, respectively (Fig. 4A). These data suggest that, as previously observed for isolated LCD/SERCA [39], refolded LCDh exists in a monomer–dimer equilibrium. On the other hand, size-exclusion chromatography of LCDΔh showed a major peak corresponding to an estimated molecular weight of 29 kDa, and no other peak at higher molecular weights, indicating that this fragment is essentially monomeric (Fig. 4B) and that the presence of the P site is essential for dimerization. These results are also in line with the studies with Na^+/K^+-ATPase described above [17,35], and altogether point to a fundamental role of P domain in self-association of P-ATPases in their native membranes. In addition, expressed LCD/Na^+,K^+-ATPase has recently been demonstrated to

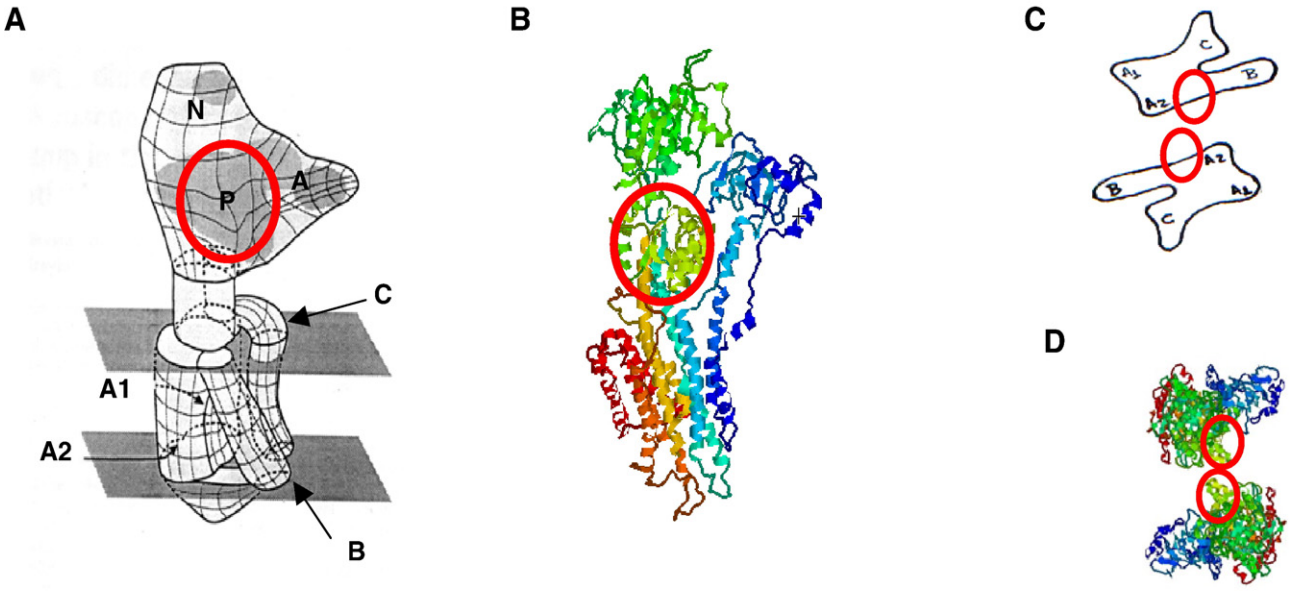

E

```
PMA     353 LAKKQAIVQKLSAIESLAGVEILCSDKTGTLTKNKLSLHEPYTVEGVSPDDLML------ 406
            +AKK AIV+ L ++E+L    ++CSDKTGTLT N++S+ + + ++ V  D   L
SERCA   326 MAKKNAIVRSLPSVETLGCTSVICSDKTGTLTTNQMSVCKMFIIDKVDGDFCSLNEFSIT 385

PMA     407 ----------------------------TACLAAS------RKKKGL-----DAIDKAF 426
                                        T C   +       + KG+     +A + A
SERCA   386 GSTYAPEGEVLKNDKPIRSGQFDGLVELATICALCNDSSLDFNETKGVYEKVGEATETAL 445

PMA     427 -------------LKSLKQYPKA-------KDALTKYKVLEFHPFDPVSKKVTAVVESPE 466
                        +++L +  +A       +  + K   LEF       +K  +V  SP
SERCA   446 TTLVEKMNVFNTEVRNLSKVERANACNSVIRQLMKKEFTLEFSR----DRKSMSVYCSPA 501

PMA     467 -------GERIVCVKGAPLFVLKTVEEDH------PIPEDVHENYENKVAELASRG--FR 511
                G ++  VKGAP  V+                P+   V E   + + E  +     R
SERCA   502 KSSRAAVGNKMF-VKGAPEGVIDRCNYVRVGTTRVPMTGPVKEKILSVIKEWGTGRDTLR 560

PMA     512 ALGVARK-------------------RGEGHWEILGVMPCMDPPRDDTAQTVSEARHLGLR 553
             L +A +                    E     +GV+  +DPPR +   ++   R  G+R
SERCA   561 CLALATRDTPPKREEMVLDDSSRFMEYETDLTFVGVVGMLDPPRKEVMGSIQLCRDAGIR 620

PMA     554 VKMLTGDAVGIAKETCRQLGL-GTNIYNAERLGLGGGGD-MPGSELADFVENADGFAEVF 611
            V M+TGD  G A   CR++G+ G N   A+R   G   D +P +E  +    A  FA V
SERCA   621 VIMITGDNKGTAIAICRRIGIFGENEEVADRAYTGREFDDLPLAEQREACRRACCFARVE 680

PMA     612 PQHKYRVVEILQNRGYLVAMTGDGVNDAPSLKKADTGIAVEGATDAARSAADIVFLAPGL 671
            P HK ++VE LQ+   + AMTGDGVNDAP+LKKA+ GIA+   T  A++A+++V
SERCA   681 PSHKSKIVEYLQSYDEITAMTGDGVNDAPALKKAEIGIAMGSGTAVAKTASEMVLADDNF 740

PMA     672 SAI 674
            S I
SERCA   741 STI 743
```

Fig. 5. Assigning the SERCA three-dimensional structure in the tubular crystal model. (A) Side view of the tubular crystal SERCA monomer model (from the opposite strand of the dimer ribbon) identifying N domain (N), A domain (A) and C-terminal portion of P domain from Asp 650 to Glu 680 (P, red circles) and the transmembrane segments, named A1, A2, B and C (arrows; scheme modified from [22]); (B) Equivalent side view using the SERCA three-dimensional structure model (1IWO); (C) Transverse cross-section of the SERCA dimer, at the lower plane in (A), identifying transmembrane segments and putative projections of the C-terminal portion of P domain of each monomer (red circles; scheme modified from [22]); (D) three-dimensional structure of (B) assigned to the dimer model of (C): top view of the cytoplasmic projection showing contact between P domain C-terminal portion of each monomer (red circles); (E) alignment between LCDh and LCD/SERCA sequences using BLAST. The arrow indicates the sequence to LCDΔh.

associate with detergent-solubilized native α-subunit [57]. As the association was stronger in the presence of MgATP for both LCD–LCD and LCD–α-subunit, N site occupancy may play a critical role in stabilizing the self-association during the catalytic cycle.

Although recent determinations of SERCA structures in two different conformations [7,8,58] showed single nucleotide-binding and phosphorylation sites, then do not exclude the possibility of ATPase–ATPase interactions, nor do they clarify the molecular basis of the regulatory site [59–61]. In fact, dimeric organizations have been described for different P-ATPase crystals in membranes [25–28]. In particular for SERCA, cryomicroscopy analysis of tubular crystals formed in native membranes revealed a dimer ribbon structure with two strands of

polarized unit, pointing in opposite directions, where the ATPase monomer from one strand is in face-to-face contact with the other through the head-shaped hydrophilic domain [22,62]. In addition, contact between adjacent P sites can also be identified in tubular crystals formed in both phosphorylated and unphosphorylated state [28]. At the time this interface could not be properly identified, due to the low resolution of the images. However, by assigning the recent high-resolution structure (E2-Tg, pdb 1IWO) with the vanadate tubular crystals, at transverse membrane level cut (Fig 5A and B), and then projecting to the cytoplasmic region, it is possible to observe that the dimer interface is formed by interaction between the C-terminal portions of P domains (Fig. 5C and D, red circles). In fact, during the final revision of the present manuscript, Hinsen and collaborators published fitting of 1IWO atomic structures into the 8 Å model [63], using a method for flexible docking of high-resolution atomic structures into electron microscopy lower-resolution densities [64]. Their results strongly corroborate the proposition that the sequence from Asp 650 to Glu 680 is positioned at the dimeric interface in such tubular crystal preparations. Comparing E1 (1SU4) and E2-Tg (1IWO) structures, it can be seen that this region remains accessible for interaction in both conformations. In agreement with these data, we propose this general dimeric model for most of P-ATPases (at least for these subclasses), taking into account that the proposed movements of N and A domains during the ion translocation mechanism are not constrained by such P-P site association. In fact, attempts to associate movements of N and A regions during the reaction cycle suggest that these two domains behave as rigid bodies, while the P domain is flexible, coordinating movements of associated transmembrane helices [65]. Thus, it is even possible to attribute subunit interplay to this plastic region of the enzyme structure.

By modeling the P site C-terminal region of several P-ATPases, it is possible to observe the presence of many hydrophobic and charged amino-acid residues at the surface (data not shown), which would favor inter-chain interactions. On the other hand, badly matched loops, due to insertion and/or deletion of amino-acid residues, might lead to specific interactions between homologous chains, especially in membranes where different ATPases are found, thus avoiding formation of non-functional heterodimers, as proposed by studies with chimeric H^+,K^+-ATPase and Na^+,K^+-ATPase α-subunits [35]. In addition, our model does not exclude formation of higher oligomeric structures, such as the hexameric structures observed with another H^+-ATPase, from *Neurospora crassa* [23,66–69]. It is possible that the regulatory domain (the C-terminal portion of H^+-ATPase chains) can alter the interaction between P-sites described here, by linking one monomer to the N domain of an adjacent chain, as proposed by Kühlbrandt et al. [68]. This effect could be dependent on phosphorylation level of the regulatory domain. Finally, our proposed model does not preclude association of other regulatory proteins such as phospholamban, which has also been proposed to associate with two Ca^{2+}-ATPase monomers [25], and to bind to Lys 393 or Lys 400 in the N domain [70,71].

Acknowledgments

We would like to thank Drs Helena Maria Scofano and Sergio Teixeira Ferreira for their valuable criticism. The paper has been kindly revised by Dr. Martha M Sorenson.

This work was supported by Coordenação de Aperfeiçoamento de Pessoal de Ensino Superior (CAPES), Conselho Nacional de Desenvolvimento Científico e Tecnológico (CNPq) and Fundação Carlos Chagas Filho de Amparo a Pesquisa do Estado do Rio de Janeiro (FAPERJ).

References

[1] S. Lutsenko, J.H. Kaplan, Organization of P-type ATPases: significance of structural diversity, Biochemistry 34 (1995) 15607–15612.
[2] J.V. Moller, B. Jull, M. le Maire, Structural organization, ion transport and energy transduction of P-type ATPases, Biochim. Biophys. Acta 1286 (1996) 1–51.
[3] J.C. Skou, The influence of some cations on an adenosine triphosphate from peripheral nerves, Biochim. Biophys. Acta 23 (1957) 394–401.
[4] D.J. Bigelow, G. Inesi, Contributions of chemical derivation and spectroscopic studies to the characterization of the Ca^{2+} transport ATPase of sarcoplasmic reticulum, Biochim. Biophys. Acta 1113 (1992) 323–338.
[5] A.N. Martonosi, The structure and interactions of Ca^{2+}-ATPase, Biosci. Rep. 15 (1995) 263–281.
[6] D.H. MacLennam, W.J. Rice, N.M. Green, The mechanism of Ca^{2+} transport by sarco(endo)plasmic reticulum Ca^{2+}-ATPases, J. Biol. Chem. 272 (1997) 28815–28818.
[7] C. Toyoshima, M. Nakasto, H. Nomura, H. Ogawa, Crystal structure of the calcium pump of sarcoplasmic reticulum at 2.6 Ă resolution, Nature 405 (2000) 647–655.
[8] C. Toyoshima, H. Nomura, Structural changes in the calcium pump accompanying the dissociation of calcium, Nature 418 (2002) 605–611.
[9] A.G. Lee, A calcium pump made visible, Curr. Opin. Struct. Biol. 12 (2002) 547–554.
[10] G. Inesi, S. Watanabe, Temperature dependence of ATP hydrolysis and calcium uptake by fragmented sarcoplasmic membranes, Arch. Biochem. Biophys. 121 (1967) 665–671.
[11] J.V. Moller, K.E. Lind, J.P. Andersen, Enzyme kinetics and substrate stabilization of detergent-solubilized and membranous (Ca^{2+}–Mg^{2+})-activated ATPase from sarcoplasmic reticulum, J. Biol. Chem. 255 (1980) 1912–1920.
[12] E. Goormaghtigh, C. Chadwick, G.A. Scarborough, Monomers of Neurospora plasma membrane H+-ATPase catalyse efficient proton translocation, J. Biol. Chem. 261 (1986) 7466–7471.
[13] J.P. Andersen, Monomer–oligomer Ca^{2+}-ATPase and the role of the subunit interaction in the Ca^{2+} pump mechanism, Biochim. Biophys. Acta 988 (1989) 47–72.
[14] J.E. Mahaney, J.P. Froehlich, D.D. Thomas, Conformation transitions of the sarcoplasmic Ca^{2+}-ATPase studied by time-resolved EPR and quenched-flow kinetics, Biochemistry 34 (1995) 4864–4879.
[15] M. Morii, Y. Hayata, K. Mizoguchi, N. Takeguchi, Oligomeric regulation of gastric H+, K+-ATPase, J. Biol. Chem. 271 (1996) 4068–4072.
[16] J.M. Merino, C. Gutiérres-Merino, F. Henao, Plausible stoichiometry of the interaction nucleotide-binding in the Ca^{2+}-ATPase from sarcoplasmic reticulum membranes, Arch. Biochem. Biophys. 368 (1999) 298–302.
[17] G. Blanco, J.C. Koster, R.W. Mercer, The α subunit of the Na,K-Atpase specifically and stably associates into oligomers, J. Biol. Chem. 91 (1994) 8542–8546.
[18] P. Maguire, K. Ohlendieck, Oligomerization of sarcoplasmic reticulum Ca^{2+}-ATPase from rabbit skeletal muscle, FEBS Lett. 396 (1996) 115–118.
[19] V. Levi, J.P.F.C. Rossi, P.R. Castello, L.G. Flecha, Structural significance of plasma membrane calcium pump oligomeric, Biophys. J. 82 (2002) 437–446.
[20] L. Dux, A.N. Martonosi, Two-dimensional arrays of proteins in

sarcoplasmic reticulum and purified Ca^{2+}-ATPase vesicles treated with vanadate, J. Biol. Chem. 258 (1983) 2599–2603.
[21] V.N. Kalabokis, J.J. Bozzola, L. Castelli, P.M.D. Hardwicke, A possible role for the dimer ribbon state of scallop sarcoplasmic reticulum. Dimmer ribbons are associated with stabilization of the Ca(2+)-free Ca-ATPase, J. Biol. Chem. 266 (1991) 22044–22050.
[22] C. Toyoshima, H. Sasabe, D.L. Stokes, Three-dimensional cryo-electron microscopy of the calcium ion pump in the sarcoplasmic reticulum membrane, Nature 362 (1993) 469–471.
[23] M. Auer, G.A. Scarborough, W. Kühlbrandt, Three-dimensional map of the plasma membrane H+-ATPase in the open conformation, Nature 392 (1998) 840–843.
[24] W.J. Rice, H.S. Young, D.W. Martin, J.R. Sachs, D.L. Stokes, Structure of Na+, K+-ATPase at 11-A resolution: comparison with Ca2+-ATPase in E1 and E2 states, Biophys. J. 80 (2001) 2187–2197.
[25] H.S. Young, L.R. Jones, D.L. Stokes, Locating phospholamban in co-crystals with Ca(2+)-ATPase by cryoelectron microscopy, Biophys. J. 81 (2001) 884–894.
[26] T. Jahn, J. Dietrich, B. Andersen, B. Leidvik, C. Otter, C. Briving, W. Kühlbrandt, M.G. Palmgren, Large scale expression, purification and 2D crystallization of recombinant plant plasma membrane H+-ATPase, J. Mol. Biol. 309 (2001) 465–476.
[27] P. Morsomme, M. Chami, S. Marco, J. Nader, K.A. Jetchum, A. Goffeau, J.-L. Rigaud, Characterization of a hyperthermophilic P-type ATPase from *Methanococcus jannaschii* expressed in yeast, J. Biol. Chem. 277 (2002) 29608–29616.
[28] F. Delavoie, D. McIntosh, F. Henao, G. Pernazi, P. Champeil, D.L. Stokes, J.-J. Lacapère, Projection map of covalently phosphorylated Ca-ATPase from tubular crystals, Ann. N. Y. Acad. Sci. 986 (2003) 17–19.
[29] T. Coelho-Sampaio, S.F. Ferreira, G. Benaim, A. Vyeira, Dissociation of purified erythrocyte Ca^{2+}-ATPase by pressure, J. Biol. Chem. 266 (1991) 22266–22272.
[30] V. Levi, J.P.F.C. Rossi, P.R. Castello, L.G. Flecha, Oligomerization of the plasma membrane calcium pump involves two regions with different thermal stability, FEBS Lett. 483 (2000) 99–103.
[31] J.D. Caviéres, Calmodulin and the target size of the (Ca^{2+}, Mg^{2+})-ATPase dependent of human red-cell ghosts, Biochim. Biophys. Acta 771 (1984) 241–244.
[32] B.J. Bowman, C.J. Berenski, C.Y. Jung, Size of the plasma membrane H+-ATPase from *Neurospora crassa* determined by radiation inactivation and comparison with the sarcoplasmic reticulum Ca2+-ATPase from skeletal muscle, J. Biol. Chem. 15 (1985) 8726–8730.
[33] D.P. Briskin, I. Reinolds-Niesman, Change in target molecular size of the red beet plasma membrane ATPase during solubilization and reconstitution, Plant Physiol. 90 (1989) 394–397.
[34] Y. Hayashi, K. Kameyama, T. Kobayashi, E. Hagiwara, N. Shinji, T. Takagi, Oligomeric structure of solubilized Na+/K(+)-ATPase linked to E1/E2 conformation, Ann. N. Y. Acad. Sci. 834 (1997) 19–29.
[35] J.C. Koster, G. Blanco, R.W. Mercer, A cytoplasmic region of the Na, K-ATPase α-subunit is necessary for specific α/α association, J. Biol. Chem. 270 (1995) 14332–14339.
[36] C. Donnet, E. Arystarkhova, K. Sweadner, Thermal denaturation of the Na, K-ATPase provides evidence for alpha–alpha oligomeric interaction and gamma subunit association with the C-terminal domain, J. Biol. Chem. 276 (2001) 7357–7365.
[37] S. Kaya, K. Abe, K. Taniguchi, M. Yazawa, T. Katoh, M. Kikumoto, K. Oiwa, Y. Hayashi, Oligomeric structure of P-type ATPases observed by single molecule detection technique, Ann. N. Y. Acad. Sci. 968 (2003) 278–280.
[38] L. Aravind, M.Y. Galperin, E.V. Koonin, The catalytic domain of the P-type ATPase has the haloacid dehalogenase fold, TIBS 23 (1998) 127–129.
[39] P.C. Carvalho-Alves, V.R. Hering, J.M.S. Oliveira, R.K. Salinas, S. Verjovski-Almeida, Requirement of the hinge domain for dimerization of Ca^{2+}-ATPase large cytoplasmic portion expressed in bacteria, Biochim. Biophys. Acta 1467 (2000) 73–84.
[40] R. Serrano, M.C. Kielland-Brandt, G.R. Fink, Yeast plasma membrane ATPase is essential for growth and has homology with (Na^+,K^+)-, K^+- and Ca^{2+}-ATPases, Nature 319 (1986) 689–693.
[41] A. Landy, Dynamic, structural and regulatory aspects of lambda site-specific recombination, Annu. Rev. Biochem. 58 (1989) 913–949.
[42] J.L. Hartley, G.F. Temple, M.A. Brasch, DNA cloning using in vitro site-specific recombination, Gen. Res. 10 (2000) 1788–1795.
[43] P. Bhandari, J. Gowrishankar, Na *Escherichia coli* host strain useful for efficient overproduction of cloned gene products with NaCl as the inducer, J. Bacteriol. 164 (1997) 4403–4406.
[44] R.A. Dohaue, R.L. Bebee, BL21-SI competent cells for protein expression in *E. coli*, Focus 21 (1999) 49–51.
[45] M.M. Bradford, A rapid and sensitive method for the quantification of microgram quantities of protein utilizing the principle of protein-dye binding, Anal. Biochem. 72 (1976) 248–554.
[46] U.K. Laemmli, Cleavage of structural proteins during the assembly of the head of bacteriophage T4, Nature 193 (1970) 680–685.
[47] N. Sreerama, R.W. Woody, Estimation of protein secondary structure from circular dichroism spectra: comparison of CONTIN, SELCON and CDSSTR methods with an expand reference set, Anal. Biochem. 287 (2000) 252–260.
[48] C. Geourjon, G. Deléage, SOPMA: significant improvement in protein secondary structure prediction by consensus prediction from multiple alignments, Comput. Appl. Biosci. 11 (1995) 681–684.
[49] V.N. Uversky, Use of fast protein size-exclusion liquid chromatography to study the unfolding of proteins which denature through the molten globule, Biochemistry 32 (1993) 13288–13298.
[50] E. Capieaux, C. Rapin, D. Thinés, Y. Dupont, A. Goffeau, Over-expression in *Escherichia coli* and purification of an ATP-binding peptide from yeast plasma membrane H+-ATPase, J. Biol. Chem. 268 (1993) 21895–21900.
[51] M.-J. Moutin, M. Cuillel, C. Rapin, R. Miras, M. Anger, A.-M. Lompré, Y. Dupont, Measurements of ATP binding on the large cytoplasmic loop of the sarcoplasmic reticulum Ca^{2+}-ATPase overexpressed in *Escherichia coli*, J. Biol. Chem. 269 (1994) 11147–11154.
[52] C. Gatto, A.X. Wang, J.H. Kaplan, The M4M5 cytoplasmic loop of the Na, K-ATPase, overexpressed in *Escherichia coli*, binds nucleoside triphosphates with the same selectivity as the intact native protein, J. Biol. Chem. 273 (1998) 10578–10585.
[53] T. Obsil, F. Merola, A. Lewit-Bentley, E. Amler, The isolated H4–H5 cytoplasmic loop of Na,K-ATPase overexpressed in *Escherichia coli* retains its ability to bind ATP, Gen. Physiol. Biophys. 17 (1998) 52–55.
[54] C.M. Tran, R.A. Farley, Catalytic activity of an isolated domain of Na, K-ATPase expressed in *Escherichia coli*, Biophys. J. 77 (1999) 258–266.
[55] P. Champeil, T. Menguy, S. Soulie, B. Jull, A. Gomez de Garcia, F. Rusconi, P. Falson, L. Denoroy, F. Henao, M. le Maire, J.V. Moller, Characterization of a protease-resistant domain of the cytosolic portion of sarcoplasmic reticulum Ca^{2+}-ATPase, J. Biol. Chem. 273 (1998) 6619–6631.
[56] B.J. Bowman, E.J. Bowman, H+-ATPases from mitochondria, plasma membranes, and vacuoles of fungal cells, J. Membr. Biol. 94 (1986) 83–97.
[57] C.J. Costa, C. Gatto, J.H. Kaplan, Interactions between Na,K-ATPase alpha-subunit ATP-binding domains, J. Biol. Chem. 278 (2003) 9176–9184.
[58] C. Toyoshima, T. Mizutani, Crystal structure of the calcium pump with a bound ATP analogue, Nature 430 (2004) 529–535.
[59] Y. Dupont, R. Pougeois, M. Ronjat, S. Verjoski-Almeida, Two distinct classes of nucleotide binding sites in sarcoplasmic reticulum Ca-ATPase revealed by 2′,3′-*O*-(2,4,6-trinitrocyclohexadienylidene)-ATP, J. Biol. Chem. 260 (1985) 7241–7249.
[60] P.C. Carvalho-Alves, C.R.G. Oliveira, S. Verjovski-Almeida, Stoichiometric photolabeling of two distinct low and high affinity nucleotide sites in sarcoplasmic reticulum ATPase, J. Biol. Chem. 260 (1985) 4282–4287.
[61] J.A. Mignaco, O.H. Lupi, F.T. Santos, H. Barrabin, H.M. Scofano, Two simultaneous binding sites for nucleotide analogs are kinetically distinguishable on the sarcoplasmic reticulum Ca(2+)-ATPase, Biochemistry 35 (1996) 3886–3891.
[62] L. Castellani, P.M. Hardwicke, P. Vilbert, Dimer ribbons in the three-dimensional structure of sarcoplasmic reticulum, J. Mol. Biol. 185 (1985) 579–594.

[63] P. Zhang, C. Toyoshima, K. Yonekura, N.M. Green, D.L. Stokes, Structure of the calcium pump from sarcoplasmic reticulum at 8 Å resolution, Nature 392 (1998) 835–839.
[64] K. Hinsen, N. Reuter, J. Navaza, D.L. Stokes, J.J. Lacapere, Normal mode-based fitting of atomic structure into electron density maps: application to sarcoplasmic reticulum Ca-ATPase, Biophys. J. 88 (2005) 818–827.
[65] N. Reuter, K. Hinsen, J.J. Lacapere, Transconformations of the SERCA1 Ca-ATPase: a normal mode study, Biophys. J. 85 (2003) 2186–2197.
[66] C.C. Cyrklaff, E. Goormaghtigh, G.A. Scarborough, 2-D structure of the *Neurospora crassa* plasma membrane ATPase as determined by electron cryomicroscopy, EMBO J. 14 (1995) 1854–1857.
[67] M. Auer, G.A. Scarborough, W. Kühlbrandt, Surface crystallisation of the plasma membrane H+-ATPase on a carbon support film for electron crystallography, J. Mol. Biol. 287 (1999) 961–968.
[68] W. Kühlbrandt, J. Zeelen, J. Dietrich, Structure, mechanism, and regulation of the Neurospora plasma membrane H+-ATPase, Science 297 (2002) 1692–1696.
[69] K.-H. Rhee, G.A. Scarborough, R. Henderson, Domain movements of plasma membrane H(+)-ATPase: 3D structures of two states by electron cryo-microscopy, EMBO J. 21 (2002) 3582–3589.
[70] C. Toyoshima, M. Asahi, Y. Sugita, R. Khanna, T. Tsuda, D.H. MacLennan, Modeling of the inhibitory interaction of phospholamban with the Ca2+ ATPase, Proc. Natl. Acad. Sci. U. S. A. 100 (2003) 467–472.
[71] H.S. Young, D.L. Stokes, The mechanics of calcium transport, J. Membr. Biol. 198 (2004) 55–63.